Resonant interatomic Coulombic decay in a laser field

C. Hoffmeister, C. Müller, and A. B. Voitkiv
Institute for Theoretical Physics I, Heinrich Heine University Düsseldorf, Universitätsstrasse 1, 40225 Düsseldorf, Germany

(Received 15 December 2021; revised 18 March 2022; accepted 21 March 2022; published 6 April 2022)

We consider photoionization in a system of two atoms of different species caused by a laser field. In this process an inner-valence vacancy, created by photoexcitation in one of the atoms, decays not only due to intra- but also interatomic electron-electron correlations with the energy release in the latter case being transferred to the other atom which is ionized. We show that when the intensity of the laser field increases this photoionization process—due to Rabi oscillations and Pauli blocking—may acquire qualitatively new features in its time evolution and the electron emission spectra.

DOI: 10.1103/PhysRevA.105.042803

I. INTRODUCTION

Even when two atoms are separated by a distance significantly longer than the typical atomic size of ~ 1 a.u. ≈ 0.53 Å, long-range electromagnetic interactions can still quite efficiently couple electrons orbiting around different atomic centers that lead to a variety of interesting physical, chemical, and biological phenomena. For example, these correlations are responsible for the energy transfer in quantum optical ensembles [1], cold Rydberg gases [2,3], and between chromophores [4].

Suppose that there are two atomic particles, A and B, which are well separated in space, and let B be in an (electronically) excited state whose excitation energy is larger than the ionization potential of A. Then the presence of particle A leads to the appearance of an additional channel for the relaxation of B since the particles can exchange the energy via two-center electron correlations. As a result of this, particle A deexcites, and particle B is ionized. Such a deexcitation mechanism can be especially efficient if particle B is initially in an excited state which can be reached from its ground state by an (electric) dipole transition. Then the energy exchange occurs via dipole-dipole transitions which possess a large effective interaction range.

In Ref. [5] the process of interatomic Auger decay was considered. In this process a vacancy in atom B is filled by one of its electrons with the energy release transferred to a neighbor atom A that ionizes the latter. The authors of Ref. [5] argued that when the two atoms are well separated in space, this process is driven mainly by the dipole-dipole interatomic coupling and showed that it can even compete with the intra-atomic (single-atom) Auger decay provided the energy release is not very large.

In Ref. [6] a system of weakly bound atomic particles with an inner-valence vacancy in one of them (say B) was considered. Because of energy constraints the vacancy could not be filled via the intra-atomic Auger process. It was predicted that the vacancy can decay due to the electron-electron interaction between B and its neighbor whose ionization potential is sufficiently small in order that the vacancy in B can be filled by transferring the energy released in B to the neighbor which is ionized. This interparticle relaxation mechanism was termed intermolecular or interatomic Coulombic decay (ICD), and this name is now widely used to denote decay mechanisms which do not necessitate an overlap between electronic shells of the interacting particles and occur via energy rather than mass and charge transfer between them.

The predictions of Ref. [6] together with advances in experimental techniques (which made it possible to observe ICD) triggered the renewed interest in mechanisms of energy transfer between atomic particles, leading to ionization, and during the past two decades various processes involving ICD in bound systems [7] as well as in atomic collisions [8] have attracted considerable attention.

In Ref. [6] it was assumed that an inner-valence vacancy is created due to emission of an inner-valence electron. If such a vacancy arises because an inner-valence electron was transferred to an excited state, its decay via the interaction with a neighbor center is termed resonant ICD (RICD) [9–12]. Depending on whether the excited electron (directly) participates or not in the energy transfer between the centers, RICD is termed participator RICD (p-RICD) or spectator RICD (s-RICD), respectively.

To our knowledge, up to now the decay of inner-valence vacancies via s-RICD triggered by photoabsorption has been studied in a weak electromagnetic field only. In such a case the role of the field is to create a vacancy after which the field becomes merely a spectator with no influence on the consequent evolution of the two-center system.

An electron, transferred by a weak electromagnetic field to an excited state, participates in the (intra-atomic) Auger decay which competes with ICD, having, thus, an indirect impact on the latter. It was also shown [13] that this electron may influence the angular distribution of electrons emitted via s-RICD. Keeping these two points in mind, in the case of a weak field this electron can, nevertheless, be regarded as a spectator since its direct impact on s-RICD remains quite modest.

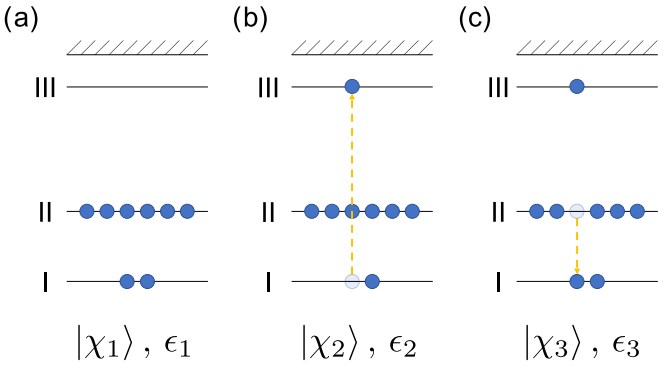

FIG. 1. Schematic of electron configurations in the ground ($|\chi_1\rangle$, ϵ_1), intermediate ($|\chi_2\rangle$, ϵ_2), and final ($|\chi_3\rangle$, ϵ_3) states, respectively, of atom B. Note that the configuration of the final state $|\chi_3\rangle$ corresponds to the s-RICD channel.

The goal of the present paper is to get some first ideas on how s-RICD can be modified if the electromagnetic field becomes more intense. The paper is organized as follows. In Sec. II we describe our approach to this problem. In Sec. III, where it is applied to a model system and to He-Ne, we discuss modifications in the time evolution and emission spectra of s-RICD, which may appear when the field becomes sufficiently intense. Section IV contains the main conclusions..

II. GENERAL CONSIDERATION

Let us consider a system consisting of two atoms A and B, which are separated by a distance R, that is sufficiently long to regard them (in the zeroth approximation) as individual particles. Initially, both atoms are in their ground-states $|\varphi_1\rangle$ with energy ε_1 (in atom A) and $|\chi_1\rangle$ with energy ϵ_1 (in atom B). The ground state of B involves a fully occupied (sub)shell I and partially or fully occupied (sub)shell II [see, for an illustration, Fig. 1(a)].

Let at time $t = t_0$ a laser field be turned on which can resonantly drive an electron from the (sub)shell I to an initially unoccupied level III of atom B [see Fig. 1(b)]. We denote by $|\chi_2\rangle$ the state in atom B with energy ϵ_2 which is formed when an electron from (sub)shell I is transferred to level III and (sub)shell II still keeps all its (initial) electrons.

Furthermore, let $|\chi_3\rangle$ be the state of atom B with energy ϵ_3 in which there is one electron on level III but (sub)shell I has restored its initial number of electrons at the expense of an electron transferred to it from (sub)shell II [see Fig. 1(c)].

We will assume that the transitions between $|\chi_1\rangle$ and $|\chi_2\rangle$ and between $|\chi_2\rangle$ and $|\chi_3\rangle$ are (electrically) dipole allowed. We will also suppose that not only the energy $\omega_{21} = \epsilon_2 - \epsilon_1$ corresponding to the transition $|\chi_2\rangle \to |\chi_1\rangle$, but also the energy $\omega_{23} = \epsilon_2 - \epsilon_3$ related to the transition between states $|\chi_2\rangle$ and $|\chi_3\rangle$ in atom B exceed the ionization potential I_A of atom A.

Once the laser field has moved an electron from subshell I to level III, an inner-shell vacancy in atom B is created that triggers various autoionization processes in the two-atom system. Indeed, the vacancy can be filled either by an electron from subshell II or by the electron from level III, and, in both these cases, the corresponding energy releases are sufficient

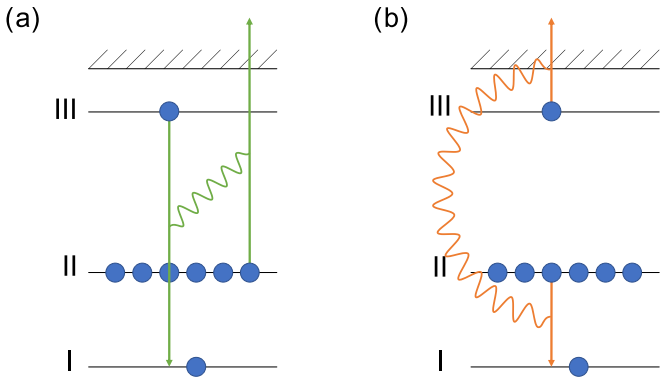

FIG. 2. Illustration of (intra-atomic) Auger decay in atom B.

for ionization of either atom. If the energy release is absorbed by atom B, the latter is ionized via (intra-atomic) Auger decay (see Fig. 2). If this energy is transferred to atom A, the latter is ionized due to ICD (p-RICD or s-RICD, see Fig. 3).

In the following we investigate the time evolution of this two-atom system driven by a resonant laser field and analyze the spectra of electrons emitted during this photoionization process.

Since normally the rates for spontaneous radiative decay are orders of magnitude smaller than Auger rates, the channels of spontaneous radiative decay will be ignored. On the other hand, the rates for direct photoionization in an intense field may be non-negligible. Therefore, we take this ionization pathway into account. However, since in what follows we will consider systems in which the direct photoionization rate for atom B is significantly larger than that for A, only direct photoionization of atom B in either its ground-state $|\chi_1\rangle$ or its excited-state $|\chi_2\rangle$ is included.

The Hamiltonian for the two-atom system in the presence of a resonant laser field then reads

$$\hat{H} = \hat{H}_A + \hat{H}_B + \hat{V}_{AB} + \hat{W}_B, \tag{1}$$

where $\hat{H}_A$ and $\hat{H}_B$ are the free atomic Hamiltonians of atoms A and B, respectively, $\hat{V}_{AB}$ is the interaction between atoms A and B and $\hat{W}_B$ is the interaction of atom B with an electromagnetic field. Treating this field as classical and assuming that it is monochromatic with frequency ω_0, we take interaction $\hat{W}_B(t)$

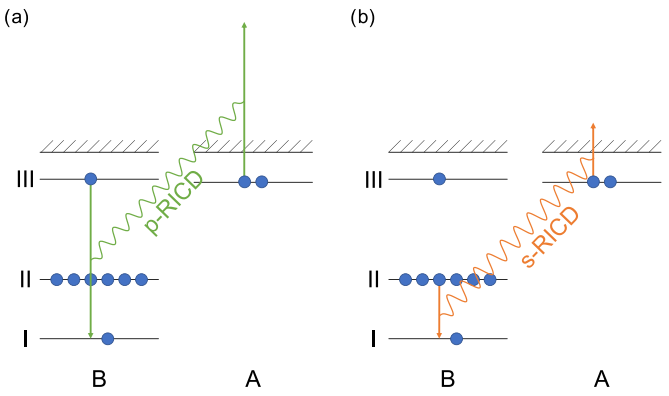

FIG. 3. Illustration of RICD channels in the system of atoms A and B: (a) participator RICD and (b) spectator RICD.

as $\hat{W}_B(t) = \hat{W}_B^0 f(t)\cos(\omega_0 t)$, where $\hat{W}_B^0$ is time independent and $f(t)$ is the laser pulse envelope function.

As it follows from the previous discussion the essential states of the two-atom system in the process under consideration include the following.

First, the ground state $|\Psi_g\rangle = |\varphi_1\rangle|\chi_1\rangle$ with energy $E_g = \varepsilon_1 + \epsilon_1$.

Second, the excited bound-state $|\Psi_e\rangle = |\varphi_1\rangle|\chi_2\rangle$ with energy $E_e = \varepsilon_1 + \epsilon_2$.

Third, the continuum states $\{|\Psi_{\boldsymbol{p}_B^a}\rangle\} = |\varphi_1\rangle\{|\chi_{\boldsymbol{p}_B^a}\rangle\}$ with energies $E_{p_B^a}$, where $|\chi_{\boldsymbol{p}_B^a}\rangle$ is the state of B in which subshell I is occupied, level III is empty, subshell II misses one electron and, due to intra-atomic Auger decay, an electron is emitted from B with asymptotic momentum $\boldsymbol{p}_B^a$, where $p_B^a = |\boldsymbol{p}_B^a| \approx \sqrt{2(\omega_0 - I_B)}$, and I_B is the ionization potential of B. We note that continuum states $\{|\Psi_{\boldsymbol{p}_B^a}\rangle\} = |\varphi_1\rangle\{|\chi_{\boldsymbol{p}_B^a}\rangle\}$ are also populated due to the direct photoionization from the ground state of atom B.

Fourth, the continuum states $\{|\Psi_{\boldsymbol{p}_A^s}\rangle\} = \{|\varphi_{\boldsymbol{p}_A^s}\rangle\}|\chi_3\rangle$ with energies $E_{p_A^s}$, which correspond to the s-RICD process, where $|\varphi_{\boldsymbol{p}_A^s}\rangle$ is the state in which an electron is emitted from A with asymptotic momentum $\boldsymbol{p}_A^s$, where $p_A^s = |\boldsymbol{p}_A^s| \approx \sqrt{2(\epsilon_2 - \epsilon_3 - I_A)}$.

Fifth, the continuum states $\{|\Psi_{\boldsymbol{p}_A^p}\rangle\} = \{|\varphi_{\boldsymbol{p}_A^p}\rangle\}|\chi_1\rangle$ with energies $E_{p_A^p}$, which are related to the p-RICD process, where $|\varphi_{\boldsymbol{p}_A^p}\rangle$ is the state in which an electron is emitted from A with asymptotic momentum $\boldsymbol{p}_A^p$, where $p_A^p = |\boldsymbol{p}_A^p| \approx \sqrt{2(\epsilon_2 - \epsilon_1 - I_A)}$.

Sixth, the continuum states $\{|\Psi_{\boldsymbol{p}'_B}\rangle\} = |\varphi_1\rangle\{|\chi_{\boldsymbol{p}'_B}\rangle\}$ with energies $E_{p'_B}$, where $|\chi_{\boldsymbol{p}'_B}\rangle$ is the state of B in which one electron is missing on subshell I (since it moved to level III) and one electron is emitted from subshell II due to direct photoionization with asymptotic momentum $\boldsymbol{p}'_B$, where $p'_B = |\boldsymbol{p}'_B| \approx \sqrt{2(\omega_0 - I'_B)}$, I'_B is the energy necessary to remove an electron from subshell II of atom B in the electron configuration described by state $|\chi_2\rangle$.

As it was already mentioned, we neglect the direct photoionization of atom A. One should also note that the direct photoionization is possible from subshell III of atom B. However, since this subshell possesses just one (and relatively weakly bound) electron, the rate for photoionization from it is much smaller than from subshell II and, therefore, neglected here.

The state vector $|\Psi(t)\rangle$ of the two-atom system then can be expanded into the set of essential states,

$$
\begin{aligned}
|\Psi(t)\rangle = {} & g(t)e^{-iE_g t}|\Psi_g\rangle + a(t)e^{-iE_e t}|\Psi_e\rangle \\
& + \int d^3\boldsymbol{p}_B^a c_{\boldsymbol{p}_B^a}(t)e^{-iE_{p_B^a}t}|\Psi_{\boldsymbol{p}_B^a}\rangle \\
& + \int d^3\boldsymbol{p}_A^s c_{\boldsymbol{p}_A^s}(t)e^{-iE_{p_A^s}t}|\Psi_{\boldsymbol{p}_A^s}\rangle \\
& + \int d^3\boldsymbol{p}_A^p c_{\boldsymbol{p}_A^p}(t)e^{-iE_{p_A^p}t}|\Psi_{\boldsymbol{p}_A^p}\rangle \\
& + \int d^3\boldsymbol{p}'_B c_{\boldsymbol{p}'_B}(t)e^{-iE_{p'_B}t}|\Psi_{\boldsymbol{p}'_B}\rangle, \qquad (2)
\end{aligned}
$$

where $g(t)$, $a(t)$, $\{c_{\boldsymbol{p}_B^a}(t)\}$, $\{c_{\boldsymbol{p}_A^s}(t)\}$, $\{c_{\boldsymbol{p}_A^p}(t)\}$, and $\{c_{\boldsymbol{p}'_B}(t)\}$ are coefficients which describe the time evolution of the system and which are to be determined.

Inserting the expansion (2) into the Schrödinger equation with the Hamiltonian given by Eq. (1) we obtain a system of coupled differential-integral equations for $g(t)$, $a(t)$, $\{c_{\boldsymbol{p}_B^a}(t)\}$, $\{c_{\boldsymbol{p}_A^s}(t)\}$, $\{c_{\boldsymbol{p}_A^p}(t)\}$, and $\{c_{\boldsymbol{p}'_B}(t)\}$ which can be solved using appropriate boundary conditions. Having obtained these coefficients one can calculate the probabilities $P_g(t) = |g(t)|^2$ and $P_a(t) = |a(t)|^2$ to find the system in the ground $|\Psi_g\rangle$ and excited $|\Psi_e\rangle$ states, respectively, the electron emission spectra, and the total populations of the continua.

In what follows we will assume that the laser field begins to act at $t = t_0 = 0$, [$g(t=0) = 1$, $a(t=0) = c_{\boldsymbol{p}_B^a}(t=0) = c_{\boldsymbol{p}_A^s}(t=0) = c_{\boldsymbol{p}_A^p}(t=0) = c_{\boldsymbol{p}'_B}(t=0) = 0$] and that its turn-on time ΔT is much shorter than the lifetimes of the two-atom system with respect to Auger and ICD decays and the inverse rate of the field-driven oscillations of atom B between states $|\chi_1\rangle$ and $|\chi_2\rangle$.

III. RESULTS AND DISCUSSION

The interaction of two bound states (say $|\chi_1\rangle$ and $|\chi_2\rangle$) with a resonant laser field results in the transfer of the population between them (the Rabi oscillations). It is the effective strength $\Gamma_f = 0.5\,|\boldsymbol{d}_{12}\cdot\boldsymbol{F}_0|$ of the coupling of these states by the laser field, which determines the period $T \sim \Gamma_f^{-1}$ of the Rabi oscillations and, thus, how fast the population moves between these states. Here, $\boldsymbol{d}_{12}$ is the transition dipole matrix element, and $\boldsymbol{F}_0$ is the amplitude of the laser field.

In the process under consideration the state $|\chi_2\rangle$ is unstable due to Auger decay and ICD (moreover, in rather intense fields, also photoionization rates for $|\chi_1\rangle$, $|\chi_2\rangle$, $|\chi_3\rangle$, and $|\varphi_1\rangle$ have to be taken into account). If the total half-width $\Gamma_t/2$ of states $|\chi_1\rangle$ and $|\chi_2\rangle$ noticeably exceeds Γ_f, then there will not be sufficient time for the population to "travel" forth and back between them due to their rapid depletion caused by decay. Such a situation is inherent to the weak-field limit of the two-atom photoionization, but it can also be encountered if the field is so intense that the photoionization rates for the states $|\chi_1\rangle$ and $|\chi_2\rangle$, which scale as $\sim F_0^2$, noticeably exceed Γ_f.

Therefore, one can expect that the most significant impact of the laser field on the time evolution and emission spectra of two-atom photoionization will be in the opposite case when the quantity Γ_f will noticeably exceed the total (half-) width mentioned above. Indeed, in such a case a vacancy in (sub)shell I of atom B will be periodically created and eliminated due to Rabi oscillations that will effectively turn on and off the channels of Auger decay and ICD.

In this section—motivated by the fact that the He-Ne dimer was actively used for the experimental and theoretical studies of ICD processes—we will consider photoionization in a He-Ne system driven by a laser field, which is resonant to the $1s^2 2s^2 2p^6 \rightarrow 1s^2 2s 2p^6 3p$ transitions in the Ne atom. One has to note, however, that, even though it is the strongest dipole allowed transition between the $2s$ and the np states in Ne, the corresponding transition matrix element turns out to be very small: $|\boldsymbol{d}_{12}| = 0.05$ a.u. This makes the condition $\Gamma_f > \Gamma_t/2$ difficult to achieve and, as a result, the increase in

the field intensity may lead to rather modest effects only (see Subsec. B).

Therefore, in order to more clearly illuminate changes in the time evolution and electron emission spectra of the photoionization process, which may appear when the laser field ceases to be very weak, we first consider this process in a model system whose parameters will be chosen to be very close to those of a He-Ne system, except the dipole matrix element $|\boldsymbol{d}_{12}|$, which will be set to 0.2 a.u.

A. Photoionization of a model two-atom system

Let our model system consist of two atoms A and B, which are weakly bound by the van der Waals force with a binding energy that is negligible compared to their ionization potentials, taken as $I_A = 24.6$ eV and $I_B = 21.6$ eV, respectively.

The atoms are irradiated by an electromagnetic field with frequency $\omega_0 \approx \omega_{21} = \epsilon_2 - \epsilon_1$ which resonantly couples the initial state $|\chi_1\rangle$ and the state $|\chi_2\rangle$ in atom B. The effective strength Γ_f of the coupling of states $|\chi_1\rangle$ and $|\chi_2\rangle$ caused by the laser field depends on its amplitude $\boldsymbol{F}_0$ and the magnitude of the transition dipole matrix element $\boldsymbol{d}_{12}$, $\Gamma_f = 0.5\,|\boldsymbol{d}_{12} \cdot \boldsymbol{F}_0|$. For our model system we choose $\omega_{21} = 45.6$ eV and $|\boldsymbol{d}_{12}| = 0.2$ a.u.

In addition to coupling states $|\chi_1\rangle$ and $|\chi_2\rangle$, the electromagnetic field makes B unstable because of photoionization of B from these states. The corresponding rates are proportional to F_0^2 and become significant when the field is sufficiently intense.

Once state $|\chi_2\rangle$ has been excited, the resulting two-atom configuration $|\Psi_e\rangle = |\varphi_1\rangle|\chi_2\rangle$ becomes unstable also because of autoionization. The corresponding decay channels include the Auger decay in atom B and two-center ICD (see Figs. 2 and 3). The Auger decay results in emission of an electron with energy $\approx \omega_0 - I_B = 24$ eV; for the corresponding Auger width Γ_B^a we take 13 meV.

In the presence of atom A, in addition to direct photoionization and Auger decay in B, two more decay channels are opened. First, the electron from level III can undergo transition back to (sub)shell I by transferring the energy $\approx \omega_0$ via two-center electron-electron correlations to atom A that leads to its ionization (the p-RICD channel). Second, provided the transition frequency $\omega_{23} = \epsilon_2 - \epsilon_3$ is larger than the ionization potential of A, the vacancy in subshell I can be filled by an electron from subshell II with the energy release transferred to atom A via ICD (the s-RICD channel). For ω_{23} and the width $\Gamma^s_{\rm RICD}$ of the s-RICD channel we will take the values of 26.6 eV and 2.7 meV, respectively.

Focusing here on the two-center photoionization involving the s-RICD process, which is of primary interest for the present paper, we will neglect the p-RICD channel. Indeed, since the ICD rates scale roughly as $1/\omega^6_{\rm icd}$, where $\omega_{\rm icd}$ is the energy transfer between the atoms, the p-RICD can be expected to be significantly weaker than the s-RICD.

We will also neglect the spontaneous radiative decay channels since, as it was already mentioned, the rates for spontaneous radiative decay are normally orders of magnitude smaller than the rates of Auger decay.

For weak laser fields, which can only very slightly deplete the population of the initial state during the pulse, the dynamics of the photoionization process is rather simple. The interaction with such a field is reduced to a single-photon exchange and the field merely creates a vacancy in (sub)shell I of atom B having essentially no effect on the two-atom system afterwards (as is typical for the s-RICD process). In particular, in weak fields the continuum population grows monotonously in time (see Fig. 4) forming a narrow maximum in the emission energy spectrum centered at the resonant energies of $\omega_{23} - I_A = 2$ eV (for s-RICD, see Fig. 5) and $\omega_0 - I_B = 24$ eV (for electron emission from atom B).

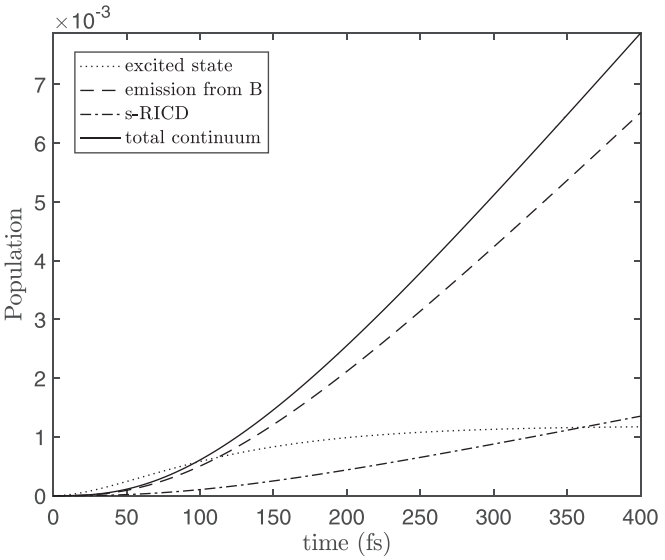

FIG. 4. The time dependence of the population of excited-state $|\Psi_e\rangle$ (dotted line), the continuum states caused by s-RICD (dashed-dot line), and electron emission from atom B (dashed line) in the weak-field case. The solid line displays the total continuum population. The population of ground-state $|\Psi_g\rangle$ remains close to 1 and is not shown.

When the intensity of the laser field increases, the dynamics of the photoionization process may significantly change

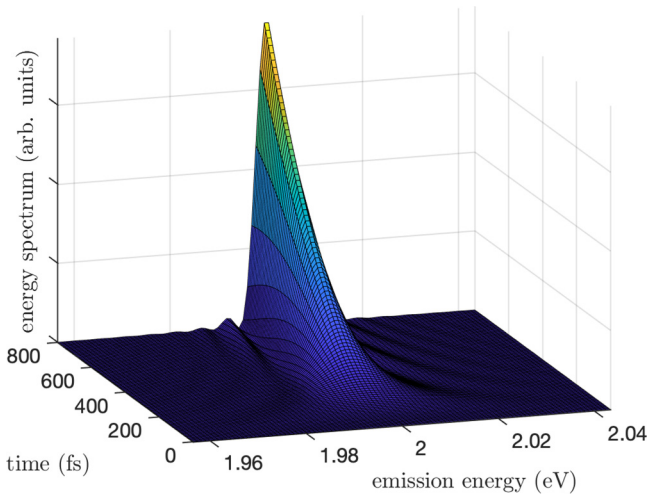

FIG. 5. The spectrum of electrons emitted via the s-RICD channel given as a function of the electron energy and time in the weak-field case.

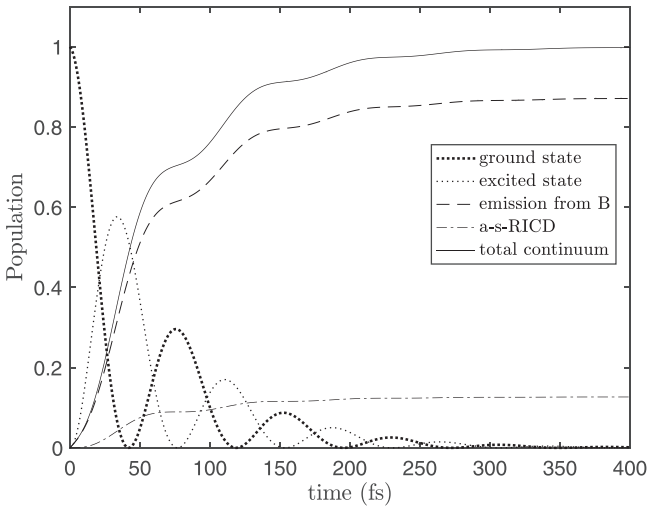

FIG. 6. The time dependence of the populations in the case of an intense laser field (the field strength $F_0 = 10^{-2}$ a.u.): Ground-state $|\Psi_g\rangle$ (bold dotted line), excited-state $|\Psi_e\rangle$ (thin dotted line), and the continuum states caused by "active-spectator" RICD (dashed-dot line), electron emission from atom B (dashed line), and the total continuum population (solid line).

acquiring qualitatively new features. Such a case is illustrated in Figs. 6, 7(a), and 7(b) for an intensity of 3.5×10^{12} W/cm^2 (the field strength is $F_0 = 10^{-2}$ a.u.). At this field intensity the effective strength Γ_f of the coupling between resonant states $|\chi_1\rangle$ and $|\chi_2\rangle$ in atom B already reaches a value of 10^{-3} a.u. $\approx$27 meV, which significantly exceeds the Auger and ICD half-widths (6.5 and 1.35 meV, respectively). At this intensity the widths of states $|\chi_1\rangle$ and $|\chi_2\rangle$ in atom B due to direct photoionization are taken to be $\approx$2.6 meV each.

The time dependence of the populations of the bound states and the continua is shown in Fig. 6. Unlike a weak field, a more intense laser field induces transitions between the initial ground $|\Psi_g\rangle$ and the excited bound $|\Psi_e\rangle$ states of the two-center system in both directions that, in the absence of the decay channels, would periodically transfer the population between them due to Rabi oscillations. Due to the Auger decay and direct photoionization in atom B and ICD, the populations of these bound states decrease with time becoming negligible already at laser pulse durations of $\gtrsim$300 fs. However, since the quantity Γ_f significantly exceeds the half-widths of Auger decay, ICD and direct photoionization, the system has enough time to perform several Rabi oscillations between the bound states before their populations vanish due to decay.

The decay channels lead to the transitions to the continuum states whose populations increase in a stepwise manner until reaching their asymptotic values at laser pulse durations where the bound states are already completely depleted by decay. The stepwise increase in the ionization probabilities is caused by the interplay between Rabi oscillations and Pauli blocking. Once the field drives the system from the ground $|\Psi_g\rangle$ into the excited state $|\Psi_e\rangle$ a vacancy in (sub)shell I of atom B is created and can be filled either by one electron from (sub)shell II or by the electron from level III that results in ICD and the Auger decay, respectively. However, the vacancy can also be filled due to the interaction with the laser field

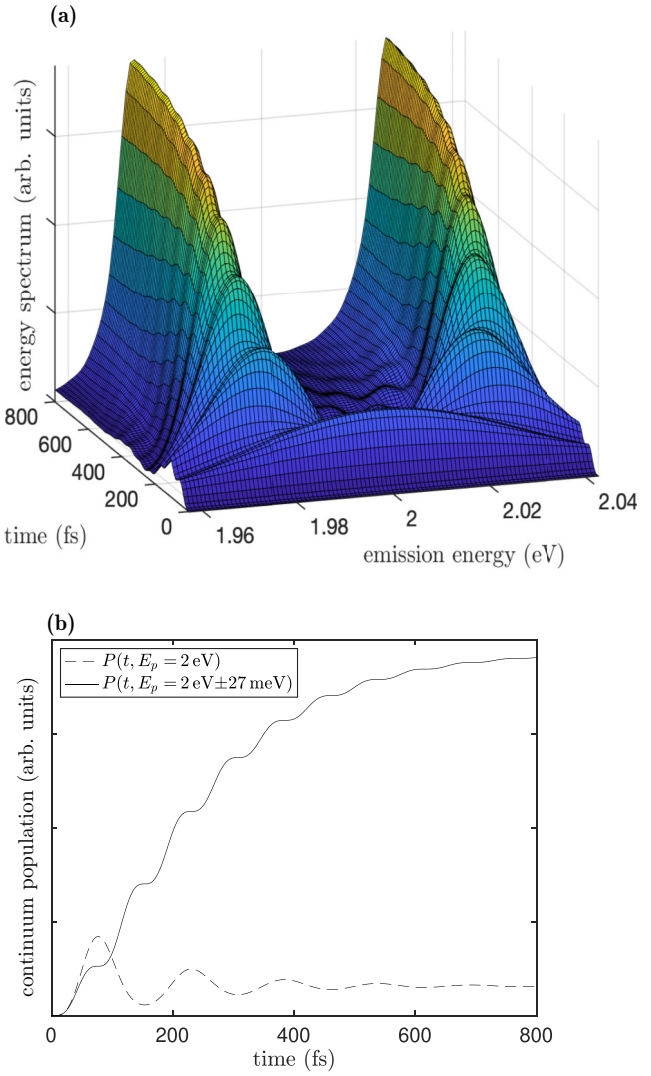

FIG. 7. (a) The spectrum of electrons emitted via the active-spectator-RICD channel given as a function of the electron energy and time. (b) The time dependence of the population of very narrow energy intervals centered at (2 ± 0.027) eV (solid line) and 2 eV (dashed line). [The energies (2 ± 0.027) and 2 eV correspond to the maxima and minimum, respectively, of the emission spectrum at large t.] For more explanations see text.

that—because of the Pauli blocking—effectively turns off the above decay channels.

As in the weak-field limit, the laser field and the electron, which is driven by this field between the resonant states, remain spectators in the sense that they do not participate in the energy exchange between the atoms. However, now both the field and the electron play a very active role by periodically turning intra- and interatomic autoionization channels on and off, this way significantly influencing the time evolution of the photoionization process. Therefore, in the considered case of intense fields the "spectator RICD" can be termed as "active-spectator RICD" (a-s-RICD).

More insight into the time evolution of the continuum population in the intense-field s-RICD can be obtained by considering the energy spectrum of the emitted electrons. It is

seen in Figs. 7(a) and 7(b) that the population not only evolves in time nonmonotonously, but also that the character of this evolution qualitatively depends on the energy of the emitted electron.

In particular, in the energy intervals where two pronounced maxima will finally be formed, the population of the continuum as a function of time shows a stepwise behavior in which time domains where the population grows are separated by intervals where it remains almost constant. After the first few significant gains the increase in the population becomes less and less pronounced until the population eventually reaches its asymptotic value.

In contrast, in the energy interval between the two maxima the spectrum shape exhibits a rather deep valley. At these energies a rapid initial increase in the continuum population is replaced by its significant decrease that leaves less than half of the preceding gain. Then the population starts to grow again (but much more smoothly) reaching a local maximum after which it slightly decreases and increases before reaching its asymptotic value.

Because of the qualitatively different character of the time evolution of the continuum population in resonant energy ranges where the pronounced maxima finally emerge and in the middle range where a deep minimum is eventually formed, the stepwise increase in the total continuum population with time is substantially less pronounced than that of the narrow energy intervals around the resonances [compare Figs. 6 and 7(b)].

To conclude this subsection we note that the stepwise increase in the total continuum population is similar to that predicted in Ref. [14] for the process of two-center photoionization in the Li-He system. However, the physics behind it is somewhat different since in the present case the Pauli blocking plays the crucial role. In addition, since the process considered here involves the "extra" state $|\chi_3\rangle$, which is not coupled by the electromagnetic field to the other bound states, the shape of the spectra of electrons emitted via the a-s-RICD qualitatively differ from that predicted in Ref. [14] possessing, for instance, a two-peak structure instead of a three-peak one inherent to the process considered in Refs. [14].

B. Photoionization of a He-Ne system

Let us consider photoionization of a He-Ne system where now He and Ne play the roles of atoms A and B, respectively. In the He-Ne dimer the He and Ne atoms are weakly bound by the van der Waals force with an equilibrium internuclear distance of 3 Å. The binding energy of the dimer ground state is only 2 meV that is much smaller than the ionization potentials of He and Ne atoms given by 24.587 and 21.564 eV, respectively.

Now states $|\varphi_1\rangle$ and $|\chi_1\rangle$ of our model represent the ground-states $1s^2$ (^1S) and $2s^22p^6$ (^1S) of He and Ne, respectively. The states $|\chi_2\rangle$ and $|\chi_3\rangle$ correspond to electronic configurations $2s2p^63p$ and $2s^22p^53p$ of Ne.

There are four states [$2s2p^63p\,(^3P_0)$, $2s2p^63p\,(^3P_1)$, $2s2p^63p\,(^3P_2)$, and $2s2p^63p\,(^1P_1)$] which can be populated by transferring an electron from the $2s$ subshell to $3p$ states. Among them state $2s2p^63p\,(^1P_1)$ possesses the largest rate (2.34×10^8 s^{-1}) for spontaneous radiative decay to the ground state [15] and, consequently, has the largest dipole transition matrix element with the ground state and will be taken to represent the $|\chi_2\rangle$ state of our model, the corresponding transition energy is $\omega_{21} \equiv \epsilon_2 - \epsilon_1 = 45.547$ eV. The value of the dipole matrix element $\boldsymbol{d}_{12}$ for the transitions between states $|\chi_1\rangle$ and $|\chi_2\rangle$, follows from the spontaneous radiative decay rate and the transition energy: $|\boldsymbol{d}_{12}| = 0.05$ a.u. Note that we extracted about the same value for $|\boldsymbol{d}_{12}|$ from experimental results of Ref. [16].

The state $2s2p^63p\,(^1P_1)$ is also unstable with respect to intra-atomic Auger decay into the $2s^22p^5\,(^2P_{1/2})$ and $2s^22p^5\,(^2P_{3/2})$ states and has the corresponding (total) Auger width Γ_a of 13 meV [16]. This width can be compared with the radiative width Γ_r of this state which is ≈ 0.15 μeV: The latter is, thus, four orders of magnitude smaller than Γ_a and can safely be neglected.

There are ten different states corresponding to an electronic configuration $2s^22p^53p$ [(i) $2s^22p^53p\,(^3S_1)$, (ii) $2s^22p^53p\,(^3D_3)$, (iii) $2s^22p^53p\,(^3D_2)$, (iv) $2s^22p^53p\,(^3D_1)$, (v) $2s^22p^53p\,(^3D_2)$, (vi) $2s^22p^53p\,(^3P_0)$, (vii) $2s^22p^53p\,(^3P_1)$, (viii) $2s^22p^53p\,(^3D_2)$, (ix) $2s^22p^53p\,(^3P_1)$, and (x) $2s^22p^53p\,(^1S_0)$] which can be populated from the $2s2p^63p(^1P_1)$ state with the respective energy release ranging from ≈ 26.58 to ≈ 27.17 eV [17]. Thus, the $2s2p^63p\,(^1P_1)$ state can decay into all these states via ICD since the energy differences are larger than the helium ionization potential $I_A \approx 24.6$ eV.

In order to estimate s-RICD rates we employed the relation [5,18],

$$\Gamma^j_{\text{s-ricd}} = \frac{3\alpha}{8\pi}\frac{c^4}{\omega_j^4}\frac{\Gamma^j_r\,\sigma^{(\text{He})}_{\text{ph}}(\omega_j)}{R^6}. \tag{3}$$

Here, c is the speed of light, Γ^j_r is the rate for spontaneous radiative decay of the jth state of Ne, where j ($j = 1, 2, \ldots, 10$) numbers the ten states corresponding to the configuration $2s^22p^53p$, ω_j is the energy transferred from Ne to He, $\sigma^{(\text{He})}_{\text{ph}}(\omega_j)$ is the cross section for He single ionization by absorption of a photon with frequency ω_j, R is the interatomic distance, which we took as the equilibrium distance of ≈ 3 Å in the He-Ne dimer and α is a numerical parameter ~ 1 which depends on the angle between the field polarization and the internuclear vector of the He-Ne system [18].

Since for all these transitions the frequencies ω_j are relatively close to each other, the photoionization cross section $\sigma^{(\text{He})}_{\text{ph}}(\omega)$ can be taken the same for all of them and using the results of Ref. [19] we obtain $\sigma^{(\text{He})}_{\text{ph}} \approx 6.59$ Mb. Using calculated rates Γ^j_r for spontaneous radiative decay [15], the total width, $\Gamma^t_{\text{s-ricd}} = \sum_j \Gamma^j_{\text{s-ricd}}$, of the two-center state $|\varphi_g\rangle\,|\chi_3\rangle$ due to the s-RICD channels was estimated to be 2.7 meV [20].

As was already mentioned, the energies and widths for the model system, which was considered in the previous subsection, were chosen to be very close to those of the He-Ne system. However, the very small magnitude of the dipole matrix element $\boldsymbol{d}_{12}$ ($|\boldsymbol{d}_{12}| = 0.05$ a.u.) for the transitions between the resonant $|\chi_1\rangle$ and $|\chi_2\rangle$ states of Ne renders the coupling of these states by the laser field much less efficient than in the case of the model system.

In order to somewhat compensate for the small value of $\boldsymbol{d}_{12}$, in our consideration of the He-Ne system, we have chosen an intensity of 1.1×10^{13} W/cm^2, corresponding to a field

strength of $F_0 = 1.75 \times 10^{-2}$ a.u. (which is by a factor of 1.75 larger that the field strength taken for the model system). With this choice we obtain $\Gamma_f = 12$ meV for the coupling between the resonant states in Ne.

One should note, however, that at $F_0 = 1.75 \times 10^{-2}$ a.u. the rates $\Gamma_{\rm ph}^{\rm Ne}$ for the decay of $|\chi_1\rangle$ and $|\chi_2\rangle$ in Ne due to photoionization reach a value of ≈ 8 meV. They, thus, become comparable to the Auger rate and already significantly exceed the s-RICD rate. We note that since the rates for the direct photo decay grow with the field strength as F_0^2 whereas the coupling parameter $\Gamma_f \sim F_0$, any further noticeable increase in the field strength leads to the condition $\Gamma_f < \Gamma_t/2$ (where Γ_t is the total decay rate) such that the system will not have time to oscillate between the bound states due to a very fast decay.

Our results for the He-Ne system are shown in Figs. 8(a) and 8(b) where we focused on the continuum energy range $\simeq 1.9934$ eV populated by electrons emitted from He via ICD involving the $2s2p^6 3p\,(^1P_1) \rightarrow 2s^2 2p^5 3p\,(^1S_0)$ transition in Ne with the corresponding ICD rate of 0.3 meV [note that this emission line is separated by about 240 meV from the nearest one related to the transition $2s2p^6 3p\,(^1P_1) \rightarrow 2s^2 2p^5 3p\,(^3P_1)$]. Compared to the model system, results for which are displayed in Fig. 7, we observe very substantial differences which are caused by the significantly smaller value of the dipole matrix element $\boldsymbol{d}_{12}$ and, consequently, the coupling parameter Γ_f. In particular, now Γ_f cannot noticeably exceed the total decay rate since the photodecay rate $\Gamma_{\rm ph}^{\rm Ne}$ grows faster with the field strength F_0 than Γ_f.

For instance, in contrast to the results shown in Fig. 7(a), in Fig. 8(a) the stepwise increase in the population of the continuum is obscure and can only be clearly observed by focusing on very narrow energy intervals [see Fig. 8(b)]. The insufficiently large magnitude of the coupling parameter Γ_f does not enable the laser field to drive an electron between the resonant states $|\chi_1\rangle$ and $|\chi_2\rangle$ several times before the Auger, ICD and photodecay already completely depleted them. Furthermore, since the coupling Γ_f between the resonant bound states is responsible for the splitting of the energy spectrum into two maxima, its modest magnitude is also behind the fact that these peaks in the spectrum shown in Fig. 8 are not well separated (which is in sharp contrast to the spectrum in Fig. 7). Moreover, the effective distance between the peaks becomes even shorter due to their significant overlap.

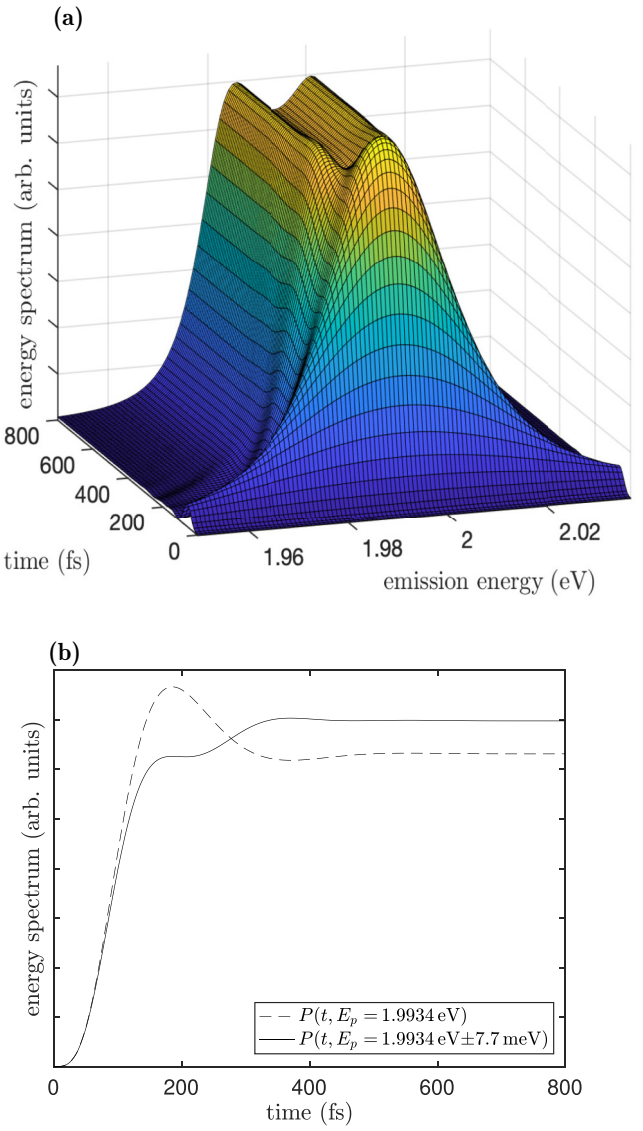

FIG. 8. (a) The spectrum of electrons emitted via the a-s-RICD channel in the He-Ne system as a function of the electron energy and time. (b) The time dependence of the population of very narrow energy intervals centered at (1.9934 ± 0.0077) eV (solid line) and 1.9934 eV (dashed line). (The energies 1.9934 ± 0.0077 and 1.9934 eV correspond to the maxima and minimum, respectively, of the emission spectrum at large t.) For more explanations see the text.

IV. CONCLUSIONS

In the "standard" s-RICD process, which occurs in a weak electromagnetic field, both an electron, transferred by photoabsorption from an inner-valence (sub)shell to an excited state, and the electromagnetic field, after having created the vacancy, become essentially merely spectators with very little influence on the consequent time evolution in the two-center system.

Here we considered how this process can be altered when the electromagnetic field becomes more intense. According to our results, at higher field intensities, an increased strength of the interaction between the former spectators—the electromagnetic field and the electron—may qualitatively change the process. Now they together may play the active role having a profound impact on the time evolution of the irradiated system and the spectra of emitted electrons. This occurs if the field-driven oscillations of the spectator electron between its initial and excited states are significantly faster than Auger decay and ICD processes. Then the oscillations periodically create and eliminate an inner-valence vacancy in one of the atoms that—due to the Pauli blocking—turns on and off the channels for Auger decay and ICD, profoundly modifying the photoionization process.

For the He-Ne system considered above such modifications turned out to be rather modest since the field-driven oscillations cannot be sufficiently rapid due to the very small dipole matrix element for the $2s \leftrightarrow 3p$ transitions. Our preliminary estimates suggest, however, that the effects discussed

in this paper can be significantly stronger in a ^{4}He-^{23}Na system [21] irradiated by a laser field resonant to the $2p^6 3s \leftrightarrow 2p^5 3s\,(^3P)\,4s$ transitions in Na.

ACKNOWLEDGMENTS

Useful input by A. Volotka and I. Tupitsyn is gratefully acknowledged [15].

[1] Z. Ficek and S. Swain, *Quantum Interference and Coherence* (Springer, Berlin, 2005).

[2] T. Amthor, M. Reetz-Lamour, S. Westermann, J. Denskat, and M. Weidemüller, Phys. Rev. Lett. **98**, 023004 (2007).

[3] E. A. Jares-Erijman and T. M. Jovin, Nat. Biotechnol. **21**, 1387 (2003).

[4] T. Förster, Ann. Phys. (Leipzig) **437**, 55 (1948).

[5] J. Matthew and Y. Komninos, Surf. Sci. **53**, 716 (1975).

[6] L. S. Cederbaum, J. Zobeley, and F. Tarantelli, Phys. Rev. Lett. **79**, 4778 (1997); R. Santra, J. Zobeley, L. S. Cederbaum, and N. Moiseyev, *ibid.* **85**, 4490 (2000).

[7] T. Jahnke, J. Phys. B: At., Mol. Opt. Phys. **48**, 082001 (2015); T. Jahnke, U. Hergenhahn, B. Winter, R. Dörner, U. Frühling, P. V. Demekhin, K. Gokhberg, L. S. Cederbaum, A. Ehresmann, A. Knie, and A. Dreuw, Chem. Rev. **120**, 11295 (2020).

[8] A. Jacob, C. Müller, and A. B. Voitkiv, Phys. Rev. A **100**, 012706 (2019); J. Phys. B: At., Mol. Opt. Phys. **52**, 225201 (2019); Phys. Rev. Research **2**, 013105 (2020); Phys. Rev. A **103**, 042804 (2021); F. Grüll, A. B. Voitkiv, and C. Müller, *ibid.* **100**, 032702 (2019).

[9] K. Gokhberg, A. B. Trofimov, T. Sommerfeld, and L. S. Cederbaum, Europhys. Lett. **72**, 228 (2005).

[10] S. Barth, S. Joshi, S. Marburger, V. Ulrich, A. Lindblad, G. Öhrwall, O. Björneholm, and U. Hergenhahn, J. Chem. Phys. **122**, 241102 (2005).

[11] K. Gokhberg, V. Averbukh, and L. S. Cederbaum, J. Chem. Phys. **124**, 144315 (2006).

[12] T. Aoto, K. Ito, Y. Hikosaka, E. Shigemasa, F. Penent, and P. Lablanquie, Phys. Rev. Lett. **97**, 243401 (2006).

[13] A. Mhamdi, J. Rist, D. Aslitürk, M. Weller, N. Melzer, D. Trabert, M. Kircher, I. Vela-Pérez, J. Siebert, S. Eckart, S. Grundmann, G. Kastirke, M. Waitz, A. Khan, M. S. Schöffler, F. Trinter, R. Dörner, T. Jahnke, and P. V. Demekhin, Phys. Rev. Lett. **121**, 243002 (2018).

[14] B. Najjari, A. B. Voitkiv, and C. Müller, Phys. Rev. Lett. **105**, 153002 (2010).

[15] In this paper we used the rates for spontaneous radiative decay of Ne states which were computed by A. Volotka and I. Tupitsyn (private communication) within the configuration-interaction Dirac-Fock-Sturm method (see I. I. Tupitsyn, V. M. Shabaev, J. R. C. López-Urrutia, I. Draganić, R. S. Orts, and J. Ullrich, Phys. Rev. A **68**, 022511 (2003); I. I. Tupitsyn, A. V. Volotka, D. A. Glazov, V. M. Shabaev, G. Plunien, J. R. C. López-Urrutia, A. Lapierre, and J. Ullrich, *ibid.* **72**, 062503 (2005); I. I. Tupitsyn, N. A. Zubova, V. M. Shabaev, G. Plunien, and T. Stöhlker, *ibid.* **98**, 022517 (2018).

[16] K. Codling, R. P. Madden, and D. L. Ederer, Phys. Rev. **155**, 26 (1967).

[17] A. Kramida, Y. Ralchenko, J. Reader, and NIST ASD Team. NIST Atomic Spectra Database (ver. 5.9), [Online]. Available: https://physics.nist.gov/asd [2021, November 28]. National Institute of Standards and Technology, Gaithersburg, MD.

[18] F. Grüll, A. B. Voitkiv, and C. Müller, Phys. Rev. Research **2**, 033303 (2020).

[19] G. V. Marr and J. B. West, At. Data Nucl. Data Tables **18**, 497 (1976).

[20] We assume for definiteness that the internuclear vector is perpendicular to the field polarization.

[21] According to calculations (see, e.g., Ref. [22]) He and Na atoms can form a very weakly bound state.

[22] U. Kleinekathöfer, M. Lewerenz, and M. Mladenovic, Phys. Rev. Lett. **83**, 4717 (1999).